Available online at www.sciencedirect.com

ScienceDirect

Energy Procedia 49 (2014) 898 – 907

Energy Procedia

SolarPACES 2013

Development of solid particle thermal energy storage for concentrating solar power plants that use fluidized bed technology

Z. Ma*, G.C. Glatzmaier, and M. Mehos

National Renewable Energy Laboratory, 15013 Denver West Parkway, Golden, Colorado 80401, USA

Abstract

The National Renewable Energy Laboratory is developing a thermal energy storage (TES) system that uses solid particles as the storage medium for a concentrating solar power plant. This paper focuses on the particle-TES performance in terms of three efficiency metrics: first-law efficiency, second-law efficiency, and storage effectiveness. The paper presents the derivation of the efficiency expression and their application in assessing the particle-TES performance and design. The particle-TES system uses low-cost stable materials that withstand high temperature at a fraction of the cost of the salt and metal containment vessels for high-temperature TES. Cost analysis indicates that particle TES costs less than $10/kWh$_{th}$, which is less than half the cost of the current molten-salt-based TES and just a fraction of liquid heat transfer fluid storage at a similar high temperature of >700°C, due to its low cost of storage medium and containment. The fluidized-bed TES can hold hot particles of > 800°C with >95% exergetic efficiency, storage effectiveness, and thermal efficiency.

Selection and peer review by the scientific conference committee of SolarPACES 2013 under responsibility of PSE AG.
Final manuscript published as received without editorial corrections.
Keywords: Concentrating Solar Power; Thermal Energy Storage; Heat Transfer Fluid; Gas/Solid Two-Phase Flow.

1. Introduction

This work estimated the cost and performance for a novel concentrating solar power (CSP) technology that uses gas/solid two-phase flow as the heat-transfer fluid and separated solid particles as the storage medium. The gas/solid particle system uses fluidized-bed technology for heat exchange and packed particles for TES. When the particle-TES is implemented in the fluidized-bed (FB)-CSP plant, the hot-solid particles discharge from the TES hot silo to

* Corresponding author. Tel.: +1-303-275-3784; fax: +1-303-630-2108.
E-mail address: zhiwen.ma@nrel.gov

Selection and peer review by the scientific conference committee of SolarPACES 2013 under responsibility of PSE AG.
Final manuscript published as received without editorial corrections.
doi:10.1016/j.egypro.2014.03.097

the FB-heat exchanger for power generation. The separated cold particles back from the power system circulate through a particle receiver for solar heat absorption and for charging the particle-TES. This paper presents the performance and design considerations for particle-TES that is integrated with a FB-CSP system. The particle-TES concept, if successfully implemented at scale, has significant advantages over the state-of-the-art two-tank molten-salt TES system.

CSP technologies that use various heat transfer fluids (HTFs), TES, and power cycles have been considered [1–16]; however, certain technology, performance, cost, or manufacturing hurdles hinder their use in CSP plants. Current state-of-the-art TES technology uses a two-tank salt system, where "hot" and "cold" tanks store the liquid salts separately. This system is used because the components associated with molten-salt handling—pumps, valves, tanks, and heat exchangers—are available at commercial scale for nitrate salts ($NaNO_3$ and KNO_3) within the salt-applicable temperature [2,3]. In a two-tank CSP system, salt flows from the cold tank to the solar receiver, is heated, and enters the hot tank. During power generation, hot salt flows to a steam generator and returns to the cold tank.

The use of FB technology and gas/solid two-phase flow to substitute for a liquid HTF provides a new approach to CSP thermal system design that can overcome many issues facing the current molten-salt-based CSP plant design, namely: salt freezing at low temperature, salt stability for high-temperature operation to support a high-efficiency power cycle, material compatibility with high-temperature containment, and high cost of both the salt and high-temperature metal structure. The particle-TES system avoids the issues of molten-salt TES with high-temperature stability (>650°C), low freezing point (<0°C), and material compatibility with high-temperature metal and non-metal materials (>650°C) at a reduced cost. The FB-CSP thermal system advances CSP thermal energy conversion and thermal storage with significant benefits in both plant cost and performance.

The FB-CSP thermal system has the potential for rapid deployment after a successful particle-receiver development, because the system leverages significant technology achievements in FB-boiler design and manufacturing approaches for a conventional power plant. The FB-CSP thermal system has high potential to transform CSP from the current expensive, performance-restricted, molten-salt-based CSP system to a low-cost, high-performance solar power plant to serve the U.S. Department of Energy (DOE) SunShot Initiative goals as well as broad solar-energy deployment.

2. FB – CSP system integration

Figure 1 shows a schematic of a FB-CSP system integrated in a CSP plant. The FB thermal system uses sensible heat of the solid particles for thermal energy storage, and has the ability to incorporate latent and thermochemical heat storage. The hot particles can be fluidized by compressed gas in a fluidized-bed (FB) heat exchanger, and the thermal energy is used for power generation as shown in Figure 1. Virtually any stable solid particles with good fluidization ability can be used as the storage media in the particle-TES. In practice, selection of particles needs to consider their stability, cost, material properties, performance of fluidization and flowability, design knowledge on heat transfer and heat exchanger, and material handling and equipment availability. In addition, the following factors are also considered in selecting solid particles for the particle-TES system:

- Consider factors regarding the overall FB-CSP thermal system performance, stability, and energy density. The particle properties relating to those factors are composition, softening temperature, density, heat capacity, particle size, and void fraction.
- Select appropriate particle sizes. Particle size is not sensitive for particle storage, but it is important for heat transfer, i.e., particle-receiver and heat-exchanger performance. Small particle size usually obtains a higher heat-transfer coefficient.
- Eventually, determine the particle size and density based on the FB-boiler manufacturer's gas/solid separator performance characteristics.

Figure 1 depicts the particle TES with the FB-heat exchanger integrated in a CSP plant with a tower solar field. The integrated FB-CSP system can drive different power-generation methods including a steam-Rankine power

cycle, or a high-efficiency supercritical carbon dioxide (s-CO_2)-Brayton power cycle. This paper focuses only on the performance analysis for a particle TES based on the TES performance metrics described in each section. The TES system assumes hot particles falling from a particle receiver on the tower top, and depleting from the bottom of a hot silo to the FB-heat exchanger. With the FB-CSP configuration in Figure 1, the cold particles out of the FB-heat exchanger reach top of the cold silo and free fall into it. The gravity-driven particle flow avoids parasitic losses in the TES system, although the particle lifting power and FB-heat exchanger parasitic power should be considered in the receiver and power block, respectively. This paper does not include the performance and design of particle receiver and FB-heat exchanger, which are under development separately. Therefore, the energy and exergy balances are only about the particle-TES system without those parasitic consumptions by the receiver and FB-heat exchanger. The FB-CSP system development leverages successful development experience from fluidization technology and attains minimum technology risk. Solid-particle TES is part of a novel FB-CSP configuration with unique particle-receiver and FB-heat-exchanger designs. The FB-CSP system provides high-temperature capability to support future high-efficiency power cycles including s-CO_2-Brayton or air-Brayton gas-turbine combined cycles. The high-efficiency power cycles can improve the CSP economics over the current CSP plants in the field.

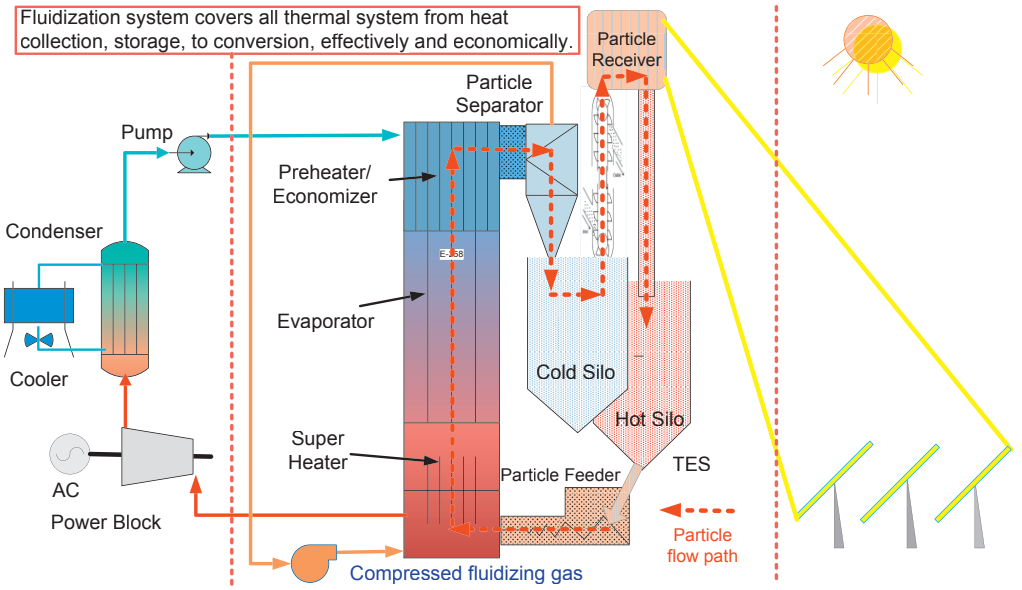

Fig. 1. Fluidized-bed CSP system with thermal energy storage.

To serve for readily-realizable power system integration, our present analysis is still based on a conventional 100-MWe steam plant with 42.5% cycle efficiency. Based on this power system assumption, we calculated 6-, 8-, 12-, and 16-hour TES storage capacities. An estimate of material and labor indicates that the FB-TES cost could be \$5–7/kWh_{th}, less than half of the DOE SunShot TES cost target of \$15/kWh_{th}. The cost number was derived from our design work involving silo concrete structure, a foundation design based on the geological condition at Barstow, California, the storage sand cost, and a preliminary insulation design. The cost estimate will be improved after insulation design and further confirmation with the material supplier and silo builder in future development.

3. Thermal energy storage performance metrics

We use the TES performance metrics with respect to three efficiencies: storage effectiveness, first-law efficiency, and second-law efficiency. The first-law efficiency of TES measures thermal losses of the storage method. The second-law efficiency reflects any reduction in exergy as storage is discharged with respect to charging conditions.

The storage effectiveness accounts for the usable portion of the gross TES media load. By capturing all of these effects systematically, we can compare various TES technologies on an equal basis before conducting more detailed simulations of the component and CSP system. The simplified modeling approach also provides preliminary design parameters and TES sizing based on a storage capacity. The method is illustrated and combined with the assessment of the particle-TES in a FB-CSP system.

3.1. Effectiveness of the FB-TES storage system

The storage effectiveness of the storage tank is sometimes called the discharge efficiency (Yang and Garimella, [16]) or the storage fraction. The storage effectiveness accounts for usable storage out of the gross TES media load. For instance, in a two-tank storage system, about 20% of the hot- or cold-tank storage fluids often remain in the tank and cannot be used due to the required pump head and for the pump needing to be submerged in the liquid. For thermocline TES, it is determined by the usable portion of the stored fluid outside the mixed-temperature thermocline region. The effectiveness of storage can be written as:

$$\eta_{eff} = \frac{Energy\ able\ to\ be\ discharged}{Total\ energy\ in\ TES} \tag{1}$$

When factoring in the storage effectiveness, a storage tank needs to be oversized to accommodate the unusable residual thermal energy.

Heated particles from a solar receiver fall into the hot silos directly through a duct. The hot silo dispenses the hot particle, as needed, from a cone-shaped bottom and is controlled by a particle-flow valve. Therefore, all hot particles can drain from the hot silo, be used for power generation, and get 100% storage effectiveness. The hot particles circulate through a fluidized-bed heat exchanger and the separated cold particles fall into the cold silo.

3.2. First-law efficiency of the FB-TES storage system

The first-law efficiency is essentially the heat loss during TES charging, discharging, and holding processes. It reflects the round-trip efficiency of the energy in and energy out of the TES. The first-law efficiency of TES systems, $\eta_{TES,\ I}$, can be defined as the ratio of the energy extracted from the storage to the energy stored in it, and can be written as:

$$\begin{aligned} \eta_{TES,I} &= \frac{Actual\ energy\ discharged}{Stored\ thermal\ energy} \\ &= \frac{m \cdot C \cdot (T - T_c)}{m \cdot C \cdot (T_h - T_c)} \end{aligned} \tag{2}$$

Where m is the total mass of the storage medium and $m{\cdot}C$ is the total heat capacity of the storage medium; T_h is the maximum temperature at the end of the charging period; T is the discharging temperature; and T_c is the cold storage media temperature. The definition of the first-law efficiency is different from Bejan ([17], p.641), where Bejan describes an indirect TES, the relation between a heater and storage media. The particle-TES integrated with a particle receiver is a direct TES system; therefore, no intermediate heat exchanger would be needed in the storage tank, so the first-law loss is mainly due to thermal losses through the storage-tank walls.

Heat loss of the TES tank consists of convection to the environment and conduction to the foundation, as shown in Figure 2, and summed in Eq. (3). The total loss is integrated over the storage time in Eq. (4).

$$\dot{Q}_{loss} = \dot{Q}_{cond,foundation} + \int_0^L p \cdot h \cdot (T_{tank}(x) - T_{env})dx + \dot{Q}_{loss,top} \tag{3}$$

$$Q_{loss,total} = \int_{t_0}^{t_f} \dot{Q}_{loss} \cdot dt \tag{4}$$

For a round tank, the perimeter is $p = 2\sqrt{\pi A}$, and A is the tank cross-section area. The heat loss from the tank side is integrated along the tank height, L, and first-law efficiency can alternatively be expressed as: $\eta_{TES,I} = Q_{loss,total}/Q_{TES}$.

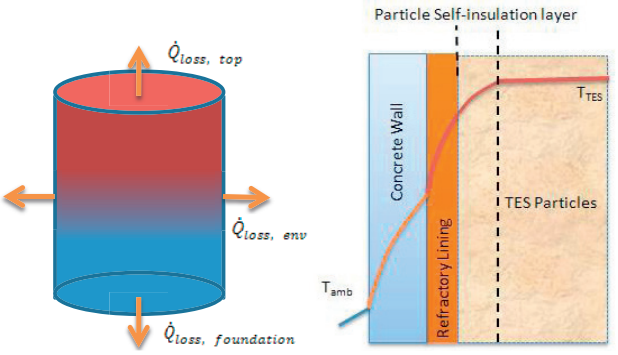

Fig. 2. TES tank heat-loss paths; self-insulation simulation.

Table 1 lists the approximate concrete and refractory thermal conductivity range. The lower particle thermal conductivity can eventually form a self-insulation layer when a thermal equilibrium is established. This self-insulation layer can prevent further heat loss over the long term (more than a day) and maintain the hot-particle temperature.

Table 1. Insulation effects comparison

Material	Thermal Conductivity (W/m-K)
Particles, k_p (sand/ash)	0.5–2 with void fraction of 0.3
Concrete, k_c	0.7–2
Refractory lining, k_r	0.2–1

Thermal insulation design for high-temperature TES is critical for both performance and cost. The storage of solid particles has many advantages over a liquid HTF by avoiding expensive alloys and potential corrosion challenges. Insulation for particle TES will be designed in conjunction with containment to accommodate an allowable concrete structure temperature. A high-temperature inner insulation liner may be used for the concrete structure thermal/mechanical requirements. Well-insulated particle containment can be realized economically by applying an exterior mineral-wool insulation layer after satisfying the applicable concrete temperature with inner insulations liner or other high-temperature materials. Future work based on available insulation materials and the need of system integration will detail the insulation design.

3.3. Exergetic efficiency of the FB-TES system

The particle TES in a FB-CSP system is sandwiched between a particle receiver and a heat exchanger for power generation, as shown in Figure 3. If an intermediate heat exchanger between the HTF and the storage media is needed, the configuration is called as indirect TES. In direct TES, HTF is the same as the storage media; therefore, no heat exchange in TES is needed. The direct TES does not incur heat-transfer exergy loss due to the absence of the intermediate heat exchanger used for an indirect TES. The only possible temperature degradation is heat losses. The external irreversibility of the receiver and heat exchanger for the power system irreversibility should not be accounted as TES exergy loss.

Exergy analyses involve several calculation steps, because no exergy property table is readily available. Our calculation refers to some analytical procedures [17, 18] and starts from basic definitions. According to Bejan ([17], 1988, p.639), the measure of indirect TES irreversibility is the second-law effectiveness of the heat exchanger:

$$\eta_{HEX,II} = \frac{Exergy\ gained\ by\ the\ cold\ stream}{Exergy\ donated\ by\ the\ hot\ stream} \tag{5}$$

Then, the TES round-trip efficiency based on exergy is written as:

$$\eta_{TES,II} = \left|\frac{\Delta G_d}{\Delta G_c}\right| = \left|\frac{(\Delta H - T_{ref}\Delta S)_d}{(\Delta H - T_{ref}\Delta S)_c}\right| \tag{6}$$

where subscripts c and d indicate TES charging and discharging processes, respectively. For an indirect storage system, $\eta_{TES,II}$ is mainly impacted by the presence of the heat exchanger between the storage media and HTF—for instance, the oil-salt heat exchanger in a trough plant. The power system heat exchanger is between the TES and power cycle, and it is categorized as either balance of plant or power block.

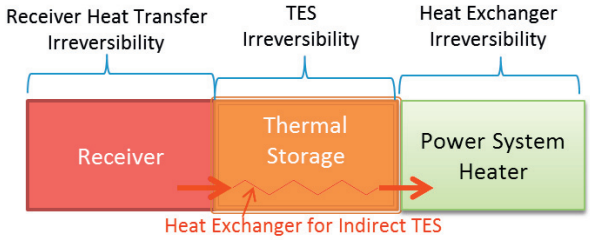

Fig. 3. Particle TES position in a FB-CSP system.

The second-law efficiency measures availability (exergy) conservation for the stored energy. The second-law energy conversion efficiency measures the energy-quality degradation due to both the difference in charging and discharging temperatures, and thermal losses [17]. It measures the conservation of exergy through the storage, i.e., the ability to generate the same amount of power from TES as from the original energy used to charge the system. Exergy transfer through a system is given as:

$$\Delta G = \Delta H - T_{ref}\Delta S \tag{7}$$

where ΔG is the exergy change of the storage fluid, the enthalpy change is $\Delta H = C \cdot \Delta T$, and $\Delta S = C \cdot \ln\frac{T_2}{T_1}$ is its entropy change. T_{ref} is the reference temperature close to ambient temperature, which is usually assumed to be 298 K (25°C) as a reference point.

Because of incorporating with a particle receiver, the FB-CSP system uses a direct TES system. Solid particles are heated directly in the particle receiver and then fall into the hot silo for storage, where the thermal storage temperature remains the particle temperature exiting the receiver. The particle-TES exergy analysis considers the exergy levels (temperature) of TES inlet particles vs. TES outlet particle temperatures. Assuming direct TES (i.e., no intermediate heat exchanger between HTF and storage media) and solid particles as both heat carrier and storage media, if there is no TES temperature drop from inlet to outlet particle temperatures, then: $T_{charge} = T_{TES} = T_{discharge}$, then the TES gets $\Delta G_d = \Delta G_c$, and $\eta_{TES,II} = 1$ and $\eta_{p,II} = 1$. For the particle-TES design presented in this paper, solid particles act as both heat carrier and storage media, and the system is well insulated with minimum thermal losses because of particle self-insulation and thick insulation layers. Thereby, theoretical exergetic efficiency could be 100% for a particle-TES.

Taking into account all potential losses, Table 3 shows the details of the exergetic efficiency and losses for particle TES. The losses include thermal losses of particle temperature degradation in the self-insulation layer, which accounts for a mere 0.2%. A granular dispenser may cause an air-cooling effect that loses less than 0.1% of energy. The particle flows down to the silo through down comer may not have loss as silo is sealed and no cold gas could be carried down.

In a double-capacity design, once the cold silo is full, the cold particles can be contained in the hot/cold dual-purpose silo, and only one cold silo needed. In this case, the hot/cold silo may be cooled by containing the cold particle and, consequently, cool the hot particles when hot particles feed in. There could be potential exergy degradation for those hot particles, and the effect is analyzed in the performance section. The loss in the hot silo when holding cold particles may be recoverable, so no exergy loss would be involved because the cold particles need to be heated anyway. Considering all losses, the total exergetic efficiency for the FB-TES still can reach 99%.

Table 2. Possible exergetic losses for particle TES.

Total loss sources	Self-insulation thickness	Down-comer and dispenser air flow	Hot silo to hold cold particles
0.9%	0.2%	0.1%	0.7%,

Following the exergy definition of Eq. (6), we calculated the FB-TES exergetic efficiency for the power-generation heat exchanger, and compared to a two-tank salt system. The exergetic efficiency for the power-generation heat exchanger, $\eta_{HEX,II}$ is shown in Table 4. The calculation is based on a steam power plant in Ref. [18] (p. 465) to provide the exergy values for the steam-generation system. We then used Eq. (6) to calculate the exergy of solid particles and salt. Table 3 shows the efficiencies relevant to integrating with a power cycle.

From the expressions of exergy change in Eq. (7), exergy, enthalpy, and entropy are functions of heat capacity temperature difference. Because the particle entropy change is small, the hot particles have higher exergy from their material properties with respect to a large temperature difference. The higher exergy (availability) in particle heat is due to its low heat capacity, resulting in a high availability for particle TES when comparing with salt as storage media. Table 3 shows the exergetic efficiency from TES to steam power generation is lower for particle due to its high availability. This efficiency is relevant to the power cycle efficiency and is different from the TES exergetic efficiency in that the efficiency is a ratio of exergy provided by the TES to the exergy consumed by the power generation. The lower $\eta_{HEX,II}$ value indicates that the particle-TES has high exergy supply, but a low-efficiency power cycle could not fully use its availability potential.

From the definition in Eq. (5), exergy efficiency for the heat exchanger is dictated by the exergy transfer from hot to cold fluid, or exergy conservation during charging and discharging processes. The calculation uses the temperature values of both the hot and cold media. The increase in temperature in the high-temperature TES reduces flow rate and maintains the same total exergy. The increase in temperature in the particle-TES reduces the particle flow rate. If no destruction of exergy occurs in the heat exchanger, a TES can maintain a high exergy transfer to the working fluid and has the ability to achieve high exergetic efficiency.

The TES exergy level and exergetic efficiency determine TES capability in driving a power cycle efficiently. The degradation of exergy due to the difference between charging and discharging temperature can be expressed in:

$$\eta_{car} = 1 - \frac{T_L}{T_H}, \text{and } \eta_{p,II} = \frac{1 - \frac{T_{ref}}{T_{discharge}}}{1 - \frac{T_{ref}}{T_{charge}}} \tag{8}$$

Eq. (8) simply expresses the Carnot cycle efficiency, and 2nd-law efficiency due to the difference between charging and discharging temperatures. The drop in discharging temperature affects the ability in supporting high-

efficiency power cycles. Table 3 compares power generation capability between the particle TES and molten-salt TES based on Carnot efficiency.

Table 3. Comparison of exergetic efficiency from TES to steam power generation.

	Particle-TES	**Molten-salt TES**
HTF T (°C)	840	560
$\eta_{HEX,II}$ (%)	78	83
η_{Car} (%)	73	64

The high-temperature TES provides the potential to obtain high Carnot-efficiency power cycles, as indicated in Eq. (8). This is the main benefit of the higher availability by high-temperature storage. The advantage of our particle-TES is its ability to drive high-temperature, high-efficiency power cycles with a potential Carnot efficiency of 73%, which is 9% higher than a 565°C salt-TES system. Achieving high efficiency relies on the high-efficiency power cycle to obtain high system efficiency. Economically, the larger temperature difference in a steam power generation system can effectively reduce the cost of an expensive superheater compared to a salt system.

In summary, the performance of the heat exchanger in the BOP for power generation depends on the power-cycle characteristics. The HTF and storage temperatures are often limited by HTF and storage capability, and unable to maintain a high exergy level. A low exergy lever limits the TES ability to drive a high-efficiency power cycle even if the heat-exchanger exergetic efficiency is high.

The high-temperature capability of particle-TES provides the potential for high-efficiency power cycles. The high-temperature particle-TES enables high electric conversion efficiency. This is in contrast to a salt-TES system, which has a temperature cap of 560°C for certain high-temperature power cycle. The particle-TES may contribute directly to cycle performance, or reduce the size and cost of a power generation system.

4. Conclusions

TES performance metrics in terms of first-law, second-law efficiencies, and storage effectiveness (or storage fraction) provide general measurement for TES design and analysis. The first-law efficiency reflects heat losses by the storage tank. The second-law efficiency indicates potential-energy conversion degradation through TES charging/discharging processes. Storage effectiveness gives the fraction of usable storage with respect to the total storage volume. Three efficiencies provide adequate performance metrics for preliminary TES design evaluations. We applied them for the new concept of fluidized-bed thermal energy storage.

The paper introduced a novel FB-CSP system using gas/solid two-phase flow to replace liquid salt or oil as HTF and solids as storage media. The materials used (ash, sand, refractory brick, and concrete) are stable, abundant, and low cost, assisting solar energy to meet the DOE SunShot cost goal. The TES can integrate with mature CFB technology for the tower system design. By collaborating with the FB-boiler manufacturer, we can develop a fluidization-based CSP thermal system by dramatically shortening the development cycle and reducing the risk. The success of the technology will be accelerated with integration of commercial fluidization technology, continued development and improvement of a solid-particle receiver, and system development of the FB-CSP plant. The FB-CSP thermal system will be compatible with any power cycle. The technology development is low risk with high return to put the product in the field.

A CSP system that operates at 600°C to more than 1000°C is possible because of stable materials and minimized thermal losses due to thermal self-insulation of particles in the storage mode. The TES can hold large-capacity thermal energy for a longer time period without the need for expensive metal alloys and insulation. The particle-TES cost in the range of \$5–\$7/kWh$_{th}$ is possible, and may achieve >75% cost reduction over the current TES—less than a quarter of the current TES cost estimated at \$30/kWh$_{th}$, or less than half of the SunShot CSP TES cost target of \$15/kWh$_{th}$—to meet the SunShot cost target on TES development. The FB-TES has the potential to support all types of power cycles, even for very high-temperature (>1000°C) needs. The uncertainty of insulation design and the associated cost may be resolved in future CSP system integration.

Nomenclature

A	Tank cross-section area, [m^2]
Bi	Biot number, hl/k [–]
c	Heat capacity, [$J/kg\ K$]
d_s	Filler particle size, [m]
E,	Energy, [J/kg]
f_{def}	Fraction of defocus, [–]
h_f	Enthalpy per unit mass, [J/kg]
h	Convection heat transfer coefficient, [$W/m^2\ K$]
k	Thermal conductivity of the solid fill [$W/m\ K$]
l	Characteristic length of the solid fill [m]
$\dot{m}$	Mass flow rate, [kg/s]
$\dot{Q}_{dem}$	Thermal load demand, [W]
$\dot{q}_A$	Available heat rate, [W]
T	Temperature, [K]
V	Volume, [m^3]

Greek letter:

η	Efficiency, [–]
ρ	Density, [kg/m^3]
ε	Packed-bed void fraction, [–]
v	Fluid kinematic viscosity, [m^2/s]

Subscripts:

c	Charge
d	Discharge
f	Fluid
htf	Heat-transfer fluid
pb	Power block
s	Solid
sf	Solar field
tes	Thermal energy storage

Superscript:

-	Average value

Acknowledgments

This work was supported by the U.S. Department of Energy under Contract No. DE-AC36-08-GO28308 with the National Renewable Energy Laboratory. The authors thank the funding support by the U.S. DOE, SunShot Initiative, under award number DE-EE0001586.

References

[1] G. Glatzmaier, "New Concepts and Materials for Thermal Energy Storage and Heat-Transfer Fluids," Technical Report NREL/TP-5500-52134, DE-AC36-08GO28308, May 20, 2011.

[2] Sandia and Bechtel Corp, "Investigation of Thermal Storage and Steam Generator Issues, Contractor Report," SAND-93-7084, 1993.

[3] B.D. Kelly, U. Herrmann, and D.W. Kearney, "Evaluation and Performance Modeling for Integrated Solar Combined Cycles Systems and Thermal Storage System," Final report on Contract RAR-9-29442-05, National Renewable Energy Laboratory, 2000.

[4] H. Price, D. Brosseau, D. Kearney, and B. Kelly, "DOE Advanced Thermal Energy Storage Development Plan for Parabolic Trough Technology," NREL Milestone Report, January, 2007.
[5] D. Bharathan and G. Glatzmaier, "Progress in Thermal Energy Storage Modeling," Proceedings of the ASME 2009 3rd International Conference of Energy Sustainability, ES2008, San Francisco, CA, 2008.
[6] D. Bharathan, "Thermal Storage Modeling," NREL Milestone Report, 2010.
[7] J. T. Van Lew, P. Li,C. L. Chan, W. Karaki, and J. Stephens, "Analysis of Heat Storage and Delivery of a Thermocline Tank Having Solid Filler Material," Journal of Solar Energy Engineering, ASME, May 2011, v. 133.
[8] J. E. Pacheco, S. K. Showalter, and W. J. Kolb, "Development of a Molten-Salt Thermocline Thermal Storage System for Parabolic Trough Plants," J. Solar Energy Engineering, v.124, pp153–159, 2002.
[9] Z. Ma, G. Glatzmaier, M. Wagner, and T. Neises, "General Performance Metrics and Applications to Evaluate Various Thermal Energy Storage Technologies," Proceedings of ESFuelCell2012, ASME Energy Sustainability Fuel Cell 2012, July, 2012, San Diego, California, USA.
[10] G. J. Kolb and V. Hassani, "Performance Analysis of Thermocline Energy Storage Proposed for the 1MW Saguaro Solar Trough Plant," Proceedings of ISEC2006, ASME International Solar Energy Conference, Denver CO, July, 2006.
[11] M. Wagner, "Simulation and Predictive Performance Modeling of Utility-Scale Central Receiver System Power Plants," Master Thesis, University of Wisconsin-Madison, December, 2008.
[12] A. McMahan, "Design and Optimization of Organic Rankine Cycle Solar-Thermal Power Plants," Master Thesis, University of Wisconsin-Madison, August, 2006.
[13] National Renewable Energy Laboratory, "SAM Manual."
[14] P. Schwarzbözl, D. Zentrum, für Luft und Raumfahrt e.V A, "TRNSYS Model Library for Solar Thermal Electric Components (STEC)," Reference Manual Release 3.0, DLR, D-51170 Köln, Germany, November 2006.
[15] TRNSYS, A Transient Simulation Program, Vers. 16, Solar Energy Laboratory, University of Wisconsin, Madison, 2006.
[16] Z. Yang and S. V. Garimella, "Molten-Salt Thermal Energy Storage in Thermoclines under Different Environmental Boundary Conditions," Applied Energy 87 (2010) 3322–3329, Elsevier.
[17] A. Bejan, *Advanced Engineering Thermodynamics*, Wiley, 1988.
[18] W. Black and J. Hartley, *Thermodynamics*, 2nd edition, HarperCollins Publishers, 1991.